Titan's planetary boundary layer structure at the Huygens landing site

Tetsuya Tokano, Francesca Ferri, Giacomo Colombatti, Teemu Mäkinen, Marcello Fulchignoni

Titan's planetary boundary layer structure at the Huygens landing site

Tetsuya Tokano,[1] Francesca Ferri,[2] Giacomo Colombatti,[2] Teemu Mäkinen,[3] and Marcello Fulchignoni[4]

Received 28 February 2006; revised 6 April 2006; accepted 10 May 2006; published 23 August 2006.

[1] Huygens Atmospheric Structure Instrument (HASI) for the first time performed an in situ measurement of the thermal structure in Titan's atmosphere with a vertical resolution sufficient to analyze the planetary boundary layer (PBL). The vertical potential temperature profile reveals the presence of a weakly convective PBL, with a surface layer thickness of 10 m and an outer layer with a depth of 300 m. With a mean eddy diffusivity of only $\sim 7.4 \times 10^{-3}$ m^2 s^{-1}, the turbulence in the PBL is weak. The turbulent heat flux in the surface layer was upward but tiny ($\sim$0.02 W m^{-2}), indicating that the ground surface was marginally warmer than the air. The surface heat flux is too small to cause a diurnal variation of the PBL except in the lowest few meters, so the observed profile may be a nearly steady state feature within this season at the landing site. In the surface layer the mean wind speed is likely to be less than 0.1 m s^{-1}. Given the tiny surface heat flux, the buoyant production of turbulence is very weak. The PBL structure reveals that the weather condition at the time and place of the Huygens landing resembles a calm, overcast day on Earth but is clearly different from the PBL typical for the polar night.

Citation: Tokano, T., F. Ferri, G. Colombatti, T. Mäkinen, and M. Fulchignoni (2006), Titan's planetary boundary layer structure at the Huygens landing site, *J. Geophys. Res.*, *111*, E08007, doi:10.1029/2006JE002704.

1. Introduction

[2] The planetary boundary layer (PBL) is the lowermost portion of the atmosphere that is affected by surface friction. The study of the PBL structure is relevant because it controls the surface- atmosphere exchange of energy, momentum and matter, thus affecting the meteorology and exogenous geology. Not surprisingly, the PBL is not unique to the terrestrial atmosphere, but ought to exist in any planetary atmosphere bounded by a solid or liquid surface. The behavior of the Martian PBL was investigated by landers [*Zurek et al.*, 1992; *Larsen et al.*, 2002; *Smith et al.*, 2004]. It was shown that generally Earth-like boundary layer meteorology is found on Mars, except that the diurnal variation is much more vigorous. The PBL on Venus measured by the Vega 2 lander has a stable stratification down to the surface [*Linkin et al.*, 1986].

[3] Titan is another accessible solid body "planet" in the solar system surrounded by a dense atmosphere on which a PBL can be expected to exist. The first crude information on Titan's PBL was provided by the radio occultation experiment of Voyager 1 [*Lindal et al.*, 1983]. The vertical temperature profile near the equator retrieved showed a lapse rate of 1.38 K km^{-1} below about 3.5 km and an abrupt drop to 0.9 K km^{-1} above this level. The lapse rate below 1 km in the evening profile (ingress) was slightly larger than in the morning profile (egress). Hence the surface may have had a slight cooling effect on the atmosphere during the nighttime. However, the temperature retrieval from the refractivity data suffered from the uncertain atmospheric composition, so any statement about the depth of the PBL on the basis of the Voyager data is somewhat inconclusive. Furthermore, intensity scintillations observed in the radio occultation profile were interpreted as internal gravity waves possibly driven by convection near the surface [*Hinson and Tyler*, 1983].

[4] The putative structure of Titan's PBL was examined on theoretical grounds by *Allison* [1992]. According to this assessment the depth of the PBL was estimated to be 700 m and several PBL parameters to be smaller than on Earth. Another approach to the PBL was a prediction of aeolian features on Titan by *Lorenz et al.* [1995]. They showed that the threshold speed for saltation would be higher than the friction speed, so aeolian transport was regarded rather difficult on Titan under present atmospheric conditions. However, in that study it was not considered that the wind in Titan's troposphere caused by Saturn's gravitational tide is much stronger than thought before [*Tokano and Neubauer*, 2002], which may have some influence on aeolian features. More recently *Tokano* [2005] investigated the seasonal and global variation in the surface and near-surface temperature by means of a three-dimensional GCM (general circulation model) assuming different surface properties and concluded

[1]Institut für Geophysik und Meteorologie, Universität zu Köln, Cologne, Germany.
[2]Centro Interdipartimentale Studi ed Attività Spaziali "G. Colombo", Università di Padova, Padua, Italy.
[3]Finnish Meteorological Institute, Helsinki, Finland.
[4]Laboratoire d'Etudes Spatiales et d'Instrumentation en Astrophysique, Observatoire de Paris, Meudon, France.

0148-0227/06/2006JE002704

that for a reasonable choice of surface parameters there may exist a stable PBL with an inversion layer in winter and a shallow convective PBL in summer, while another GCM predicted that the surface temperature is almost independent of season [*Rannou et al.*, 2006].

[5] The Huygens probe that descended into Titan's atmosphere on 14 January 2005 measured for the first time several meteorologically relevant quantities such as temperature and pressure [*Fulchignoni et al.*, 2005], wind [*Bird et al.*, 2005; *Tomasko et al.*, 2005] or chemical composition of the atmosphere [*Niemann et al.*, 2005]. The reversal of the wind direction from westerlies to easterlies near 7 km observed by Huygens was interpreted as evidence of entering the PBL [*Tomasko et al.*, 2005]. This comparison illustrates that the previous estimations of the PBL depth differ by one order of magnitude from each other. Recent images of Titan's surface taken by Cassini show some surface albedo streaks and other features that might point to aeolian features [*Porco et al.*, 2005]. Since the significance of aeolian feature is intimately coupled to the PBL structure there is an urgent need to analyze Titan's PBL on in situ observational basis.

[6] In this study we analyze the structure of Titan's PBL mainly on the basis of the thermal structure measured by Huygens Atmospheric Structure Instrument (HASI) [*Fulchignoni et al.*, 2005] by analogy with the terrestrial boundary layer meteorology.

2. Observational Evidence for the PBL

2.1. General Setting of the Huygens Landing Site

[7] Before analyzing the data relevant for the characterization of Titan's PBL we first briefly describe the general setting of the Huygens landing site to facilitate the meteorological interpretation of the data.

[8] The landing site of the Huygens probe on Titan is located at 10.3° ± 0.4°S, 192.3° ± 0.5°W (167.7° ± 0.5°E), in a dark area close to the boundary between a bright, icy, rugged terrain and a darker flat area [*Lebreton et al.*, 2005]. It has been interpreted as a dried lakebed and is located some 5 km to the south of highlands where fluvial features were detected [*Tomasko et al.*, 2005]. The image taken after the landing shows a flat plain strewn by small 'cobbles' presumably consisting of ice with a typical size of 15 cm. The surface material was described as solid but soft [*Zarnecki et al.*, 2005]. The solid state of the surface in contrast to a liquid surface strongly constrains the characteristics of the PBL since the heat and momentum exchange is substantially larger than in the case of liquids.

[9] The landing of Huygens on Titan took place at 14 January 2005 1138:10 UTC, corresponding to 9:47 A.M. local true solar time (LTST) at the landing site according to the algorithm by *Allison et al.* [2004]. The season of landing was L_S = 300.5°, i.e., in southern midsummer. The solar zenith angle was 34° and the subsolar point was located to the east of the landing site. An overview of the different time units used in this work is given in Table 1.

[10] The simulation of the global and seasonal variation in the surface temperature by the GCM (general circulation model) of *Tokano* [2005] shows for two solid surface types that in the season and latitude of landing both the surface and near-surface temperature are predicted to be close to the global and annual average and also very close to that at the foot points of the radio occultation profiles of Voyager 1 near the equator at L_S = 9°. Therefore the PBL structure at the Huygens site can be expected to be similar to that retrieved from Voyager 1 [*Lindal et al.*, 1983].

Table 1. Overview of Different Time Units Used in This Work[a]

Time Unit	Sunrise	Landing
Julian Date	2453381.77	2453384.98
UTC	12 Jan 2005 1830	14 Jan 2005 1138
Local true solar time (LTST)	5:42 A.M.	9:47 A.M.
Time past sunrise		
in seconds	0	2.77×10^5
in Earth days	0	3.21
in Titan days	0	0.20
Season (L_S), deg	300.5	300.5

[a]The values are valid for the Huygens landing site.

2.2. Potential Temperature Profile

[11] The most reliable and convenient signature of a PBL to be found in the vertical sounding of the atmosphere is the vertical profile of potential temperature θ. The θ profile in the PBL can markedly differ from that in the free atmosphere, and reveals the static stability of the atmosphere at a given instant, which is a major classification criterion of the PBL, while the local lapse rate alone is insufficient to determine the static stability.

[12] The meteorological data relevant for the analysis of the PBL were acquired approximately within the last minute before landing. The atmospheric temperature was measured by two independent and redundant HASI temperature sensors (TEM) mounted on a stem (STUB) to ensure appropriate positioning and orientation in the gas flow during measurement. The TEM sensors are located 140.5 mm distant from the base of the stem. The two TEM sensors measured alternately and each sensor measured with an accuracy of ±0.25 K and during the last km before touchdown the sampling interval was 2.5 s, corresponding to a height resolution of about 10 m. For the analysis in this work the temperature measured by the TEM 1 fine sensor is used. The atmospheric pressure was measured by the HASI Pressure Profile Instrument (PPI) also mounted on the stem, and the entering hole of the Kiel probe is located approximately 205 mm from the base of the stem. PPI measures with an accuracy of ±1 hPa and a sampling interval of about 4.7 s. For the altitude reconstruction from the measured time series the real gas equation (virial equation) was used considering the atmospheric composition measured by Huygens GCMS (Gas Chromatograph Mass Spectrometer) [*Niemann et al.*, 2005], as described in *Mäkinen* [1996]. Since the temperature and pressure were not measured simultaneously the pressure values from PPI are interpolated to the altitudes of temperature measurements of TEM 1 fine sensor. The measured vertical profile of temperature and pressure in the lowest 1 km are shown in Figure 1.

[13] The potential temperature θ is defined as

$$\theta = T\left(\frac{p_0}{p}\right)^{(c_p - c_v)/c_p} \quad (1)$$

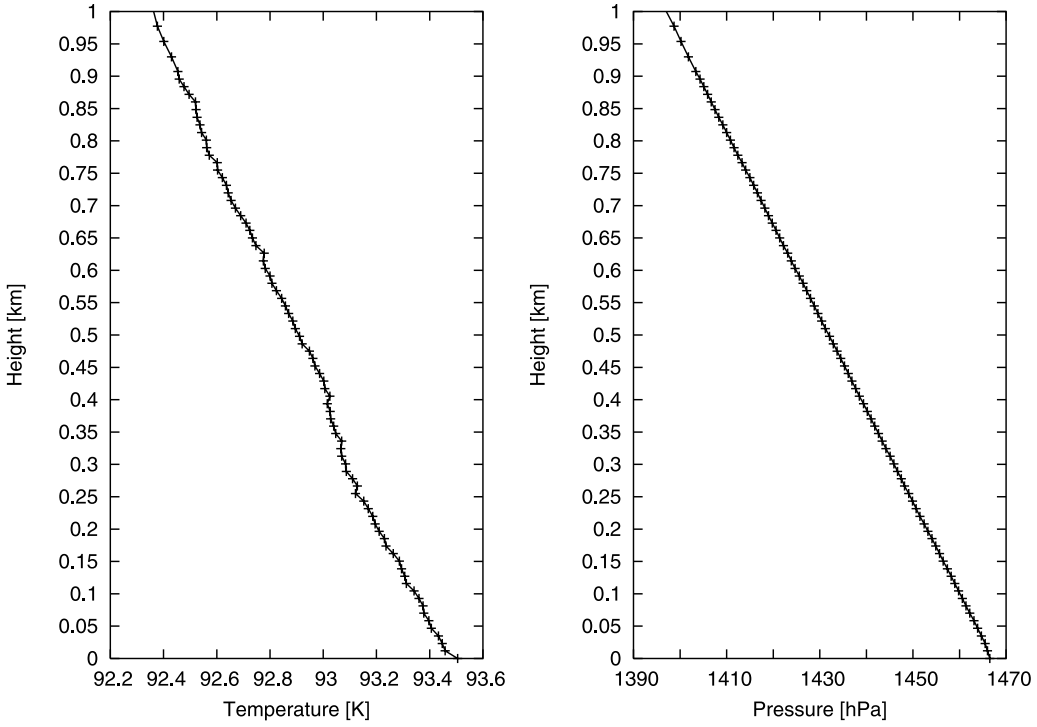

Figure 1. (left) Vertical profile of temperature measured by TEM 1 fine sensor in the lowest 1 km. (right) Vertical profile of pressure measured by the PPI sensor. Temperature and pressure profiles at higher altitudes can be found in work by *Fulchignoni et al.* [2005].

where T is the temperature, p_0 is the reference pressure, p is the pressure at a level under consideration, c_p is the specific heat capacity at constant pressure and c_v is the specific heat capacity at constant volume.

[14] The reference pressure is taken to be the mean surface pressure measured after the landing (p_0 = 1467.2 hPa). For calculating the specific heat capacities the atmospheric composition near the surface measured by Huygens GCMS [*Niemann et al.*, 2005] is adopted, i.e., 95.1% N_2, 4.9% CH_4 and no Ar. Using the ideal gas equation the corresponding c_p and c_v near the surface with this atmospheric composition is 1204.5 J K^{-1} kg^{-1} and 824.5 J K^{-1} kg^{-1}, respectively, with the exponent in equation (1) being 0.3063. Using the real gas equation (virial equation) [*Mäkinen*, 1996] they amount to c_p = 1103.5 J K^{-1} kg^{-1} and c_v = 760.5 J K^{-1} kg^{-1}, with the exponent being 0.3108. However, the difference between θ calculated with these different specific heat capacities is negligible in the lower troposphere. For instance at 300 m the difference is only 0.006 K, much smaller than the error bar of θ resulting from errors in T, p or methane mixing ratio.

[15] Figure 2 shows the vertical profile of θ in the lowermost part of the troposphere in two different scales. At the immediate surface θ slightly decreases from 93.52 K at the surface down to 93.48 K within the lowest ∼10 m. θ then virtually stays constant up to 300 m. Above 300 m the potential temperature gradient becomes positive, with an average gradient of $\gamma \sim 4 \times 10^{-4}$ K m^{-1}. However, a well-defined capping inversion, i.e., a positive jump of θ at the top of the PBL, cannot be recognized. The potential temperature calculated with the redundant temperature data from TEM 2 fine sensor virtually exhibits the same vertical profile, with a tiny offset (0.09 K), so this observed structure is reliable.

[16] The presence of a negative θ gradient near the surface, constant θ for some altitude and positive gradient on top of it can only be interpreted as a convective PBL according to the PBL classification shown in Figure 5.17 of *Stull* [1988]. In this case the static stability is slightly unstable in the entire PBL. The lowermost part in which θ decreases as altitude increases is referred to as the surface layer, and is characterized by a vertically constant flux of heat and momentum. In a convective PBL the upper boundary of the PBL is defined as the altitude at which θ exceeds the surface θ for the first time. In Figure 2 θ begins to increase and exceeds the surface θ near 300 m, so this may be regarded as the depth of the PBL at the Huygens site at the time of landing. With a surface pressure of 1467.2 hPa and a pressure of 1446 hPa at 300 m the PBL contains roughly 1% of the total atmospheric mass. The depth of the surface layer constitutes only 3 to 4% that of the entire PBL, somewhat smaller than in a typical terrestrial PBL (10%). Although the wind direction reverses near 7 km and this was interpreted as the top of the PBL [*Tomasko et al.*, 2005], we cannot recognize any qualitative or quantitative change in the θ profile between 5 and 10 km. For this reason we do not regard 7 km as the depth of the PBL at the landing site on the basis of our data.

[17] The convective character of the observed PBL is only marginal considering the tiny vertical gradient of θ near the surface. Even a decrease of the surface θ by 0.1 K would turn the surface layer into a slightly stable state and the outer layer will then be mechanically decoupled from the surface layer by virtue of weakening the turbulence. However, the presence of

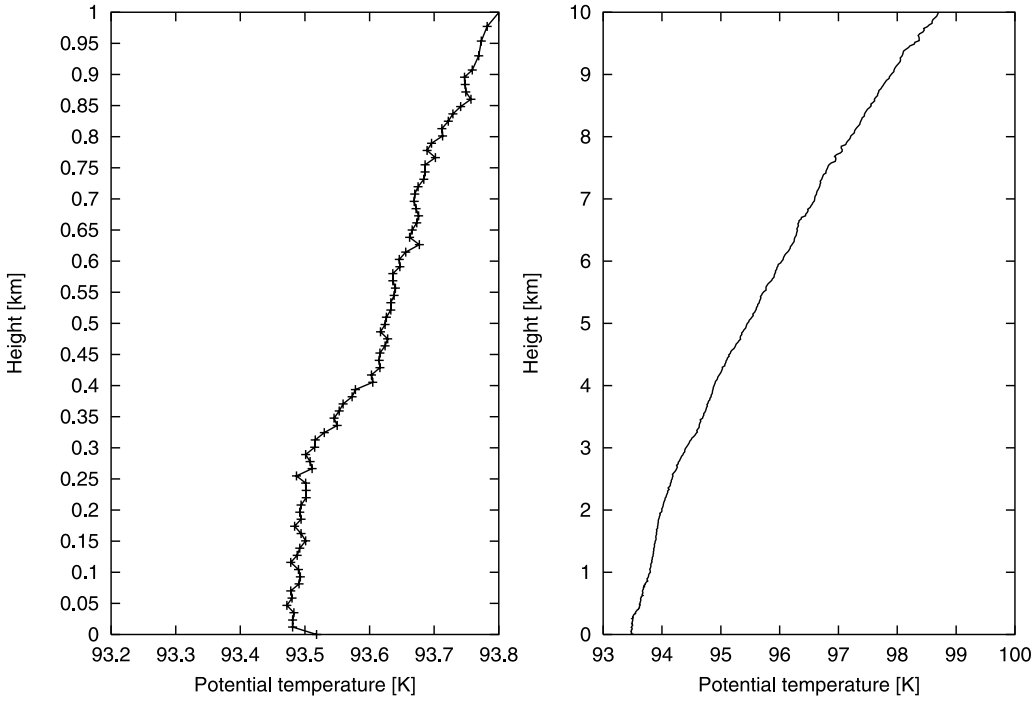

Figure 2. Vertical profile of potential temperature θ in two different scales: (left) lower 1 km and (right) lower 10 km. The temperature data are obtained from TEM 1 fine sensor, and θ is calculated from temperature and pressure data considering the atmospheric composition measured by Huygens GCMS [*Niemann et al.*, 2005]. The tics in the left plot mark the altitudes at which the temperature data were acquired. Pressure data are interpolated to the temperature levels. The error bar for θ is ∼0.3 K.

such a diurnal cycle will essentially depend on whether the ground can respond to diurnal forcing and the heat is efficiently exchanged between the atmosphere and surface, and will be investigated in section 4.

3. Dynamical Parameters of the PBL

[18] The potential temperature profile shown in Figure 2 represents one major data set that can be used to constrain various parameters of the PBL for the place and time of landing.

3.1. Eddy Diffusivity

[19] In a simple analytic model describing the outer layer of the PBL the turbulence expressed in terms of the eddy diffusivity is related to the mixed layer depth D [e.g., *Stull*, 1988] via

$$D = \pi\sqrt{\frac{2K}{f}} \tag{2}$$

where K is the eddy diffusivity and f is the Coriolis parameter (1.63×10^{-6} s^{-1} for the latitude of 10.3°S at the Huygens landing site).

[20] With a D of about 300 m the eddy diffusivity amounts to $K \sim 7.4 \times 10^{-3}$ m^2 s^{-1}, roughly one order of magnitude smaller than previously estimated (0.1 m^2 s^{-1} by *Flasar et al.* [1981]). It should be noted that this value is specific to the Huygens landing site where the Coriolis parameter is particularly small.

[21] At higher latitudes, i.e., with a larger Coriolis parameter, the PBL depth would be shallower for a given eddy diffusivity. For instance at 60° latitude (Coriolis parameter of 7.9×10^{-6} s^{-1}) the PBL depth would be shallower than at the Huygens site by a factor of 2.2. Alternatively an eddy diffusivity about 5 times larger than at the Huygens site would be required at 60° latitude to sustain the same PBL depth (300 m).

3.2. Surface Roughness Length

[22] The surface roughness length z_0 is a geometric characteristic of a surface with its efficiency as a momentum sink for turbulent flow. An empirical formula for the surface roughness length for a plain strewn by rocks was provided by *Lettau* [1969]

$$z_0 = 0.5 H_z \frac{H_z H_x}{A} \tag{3}$$

where H_z is the average height of the roughness elements, H_x is the horizontal width of the same and A is the average surface area per rock, i.e., total area divided by the number of rocks. This formula was developed for the terrestrial PBL, but has also been applied to the PBL of Mars [e.g., *Larsen et al.*, 2002].

[23] For the Huygens landing site the image taken after the landing [*Tomasko et al.*, 2005, Figure 4] may be used. According to analyses of this image typically H_x is 15 cm, H_z is 10 cm and A is ∼1/6 m^{-2}. With these values we estimate z_0 to $\sim 5 \times 10^{-3}$ m.

[24] The surface roughness length can be correlated to the surface drag coefficient C_D via

$$C_D = \frac{k^2}{\ln\left(\frac{z}{z_0}\right)^2} \tag{4}$$

where $k = 0.4$ is the von Kármán constant, z is 10 m by definition in boundary layer meteorology [*Stull*, 1988].

[25] This estimation yields $C_D = 0.0028$ characteristic of such a plain consisting of solid material. C_D smaller than 0.001 is unlikely in the absence of a liquid surface and C_D larger than 0.005 is also unlikely in the absence of vegetation or high topography. However, we note that z_0 and C_D may considerably vary across Titan. For instance Cassini radar observations seem to indicate that the bright Xanadu region is rougher than the dark terrain surrounding it [*Elachi et al.*, 2005]. Very small values corresponding to liquid surface are not representative of Titan anywhere because there is no evidence of oceans on Titan [*West et al.*, 2005]. Possible presence of small lakes would not drastically change these values.

3.3. Friction Speed

[26] The friction speed u_* is a PBL parameter characterizing the strength of the surface wind stress. We estimate the friction speed from the eddy diffusivity, surface layer depth and surface roughness length using one of the matching conditions between the surface layer and outer layer [*Haltiner and Williams*, 1980]

$$K = ku_*(h + z_0) \tag{5}$$

where $h = 10$ m is the surface layer depth, $z_0 = 5 \times 10^{-3}$ m is the surface roughness length.

[27] From this relation u_* is determined as 1.9×10^{-3} m s^{-1}. The corresponding surface stress is $\tau = \rho u_*^2 = 1.9 \times 10^{-5}$ N m^{-2}, where $\rho = 5.4$ kg m^{-3} is the air density at the surface calculated from the measured temperature and pressure. The derived friction speed is smaller than typical terrestrial values (0.3 m s^{-1}). On the other hand, this estimation is consistent with the friction speed estimated by *Lorenz et al.* [1995] using their formulation $u_* = \sqrt{v_0 v_r C_D} \sim 3 \times 10^{-3}$ m s^{-1}, where $v_0 = 3 \times 10^{-4}$ m s^{-1} is the heat transport speed, $v_r = 11.6$ m s^{-1} is the circumferential speed of Titan at the equator and $C_D = 0.002$ is the surface drag coefficient they assumed (which is realistic according to our analysis in section 3.2).

3.4. Wind Profile in the Surface Layer

[28] In the surface layer where the vertical momentum flux is regarded as constant with height and the Coriolis force is treated negligible the vertical profile of the horizontal wind can be approximated by the logarithmic wind profile

$$u = \frac{u_*}{k}\ln\left(\frac{z}{z_0}\right) \tag{6}$$

Figure 3 shows the logarithmic wind profile calculated with the parameters derived above. The wind speed rapidly increases from zero at the surface to ~0.04 m s^{-1} at the top of the surface layer (10 m). The wind direction cannot be determined solely from the information we gather from the thermal structure of the PBL. This result is consistent with the estimation of near-surface winds in the lowest meter of the atmosphere of 0.2 m s^{-1} or probably much less on the basis of the analysis of the cooling behavior by ventilation of the landed Huygens probe [*Lorenz*, 2006].

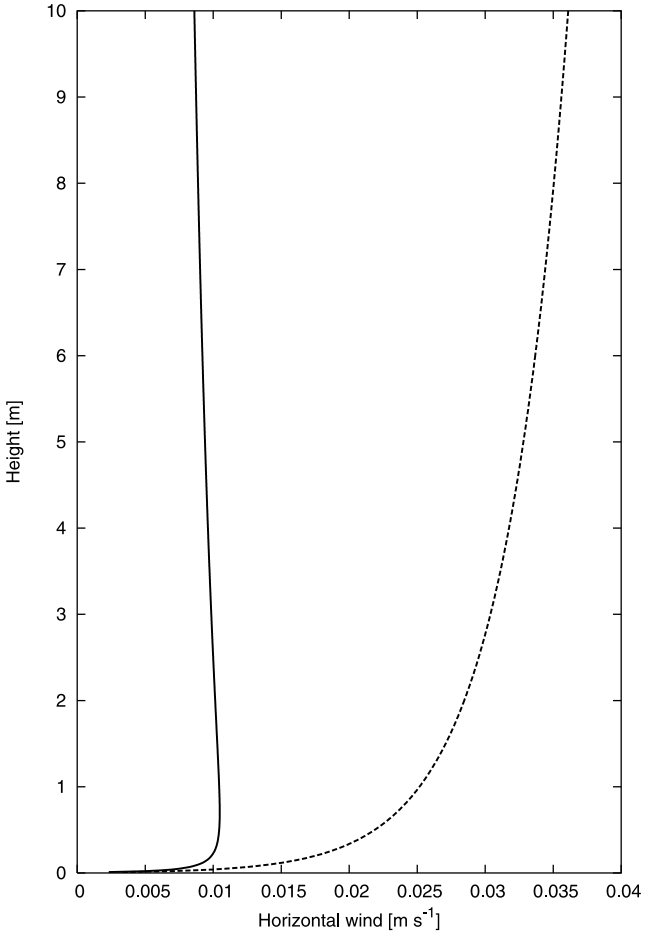

Figure 3. Putative mean wind profile in the surface layer calculated with the PBL parameters derived from the potential temperature profile. The wind direction should not change within the height region shown here. The dashed line is the pure logarithmic profile neglecting the similarity function, while the solid line is the wind profile corrected with the similarity function for unstable condition.

[29] However, since the stratification in the surface layer is slightly unstable the logarithmic wind profile has to be modified according to the Monin-Obukhov similarity theory [e.g., *Stull*, 1988] as

$$u = \frac{u_*}{k}\left[\ln\left(\frac{z}{z_0}\right) - \Psi_m\left(\frac{z}{L}\right)\right] \tag{7}$$

where Ψ_m is the similarity function which is a sole function of the stability parameter z/L.

[30] Here L is the Obukhov length defined as

$$L = \frac{-u_*^3}{k\frac{g}{\theta_0}\overline{w'\theta'}} \tag{8}$$

With the parameters already determined above and the kinematic heat flux $\overline{w'\theta'}$ defined in section 4.1, L turns out to be -0.32 m.

[31] The similarity function is

$$\Psi_m\left(\frac{z}{L}\right) = \ln\left[\left(\frac{1+x^2}{2}\right)\left(\frac{1+x}{2}\right)^2\right] - 2\tan^{-1}x + \frac{\pi}{2} \tag{9}$$

where $x = (1-15\ z/L)^{0.25}$.

[32] The resulting wind profile in the surface layer is also shown in Figure 3 for comparison. This profile exhibits a sharp increase only in the lowest 20 cm and above this height it remains almost constant at 0.01 m s^{-1} up to the top of the surface layer, with a negative deviation from the logarithmic profile. Given the uncertainty in some of the parameters it is reasonable to assume that the mean wind profile is likely to be located between these two profiles.

[33] Essentially the steepness of the wind profile depends on the friction speed, surface roughness parameter and the Obukhov length. However, a characteristic feature of the surface layer is the height-independent wind direction. The reason for the unidirectional wind in the surface layer is the negligible influence of Coriolis force in this portion of the PBL. Therefore the wind direction at the surface is the same as at 10 m above the surface.

[34] The wind profile in the outer PBL above 10 m is a more complex issue, and will not be treated in this paper; this could be better analyzed in conjunction with the wind data measured by the Doppler Wind Experiment (DWE) [*Bird et al.*, 2005] and Descent Imager Spectral Radiometer (DISR) [*Tomasko et al.*, 2005], which is beyond the scope of this study.

4. Heat Budget in the PBL

4.1. Surface Heat Flux

[35] The surface (sensible and latent) heat flux is one relevant component in the surface energy budget, along with absorption and reflection of radiation at the surface and heat conduction in the soil. The sensible heat flux is equivalent to the convective heat flux used in energy balance models. There is no method for directly measuring the surface heat flux [*Arya*, 2001]. On the other hand, the observed θ profile can be thought of as a result of vertical heat flux at the surface. The surface heat flux can be estimated from the θ profile and the friction speed under the assumption that the heat flux is height-independent within the surface layer.

[36] In the Monin-Obukhov similarity theory the potential temperature in the surface layer obeys a logarithmic profile

$$\theta = \theta_0 + \frac{\theta_*}{k}\left[\ln\left(\frac{z}{z_0}\right) - \Psi_h\left(\frac{z}{L}\right)\right] \tag{10}$$

Here, θ_0 is the potential temperature on the surface and θ_* is the turbulent temperature scale, a factor determining the steepness of the logarithmic θ curve that can be estimated from the observed θ curve. $\Psi_h = 2\ \ln(\frac{1+x^2}{2})$ is the similarity function for heat, but in deriving θ_* we neglect Ψ_h since L hidden in Ψ_h itself is a function of the unknown (θ_*) we are seeking for. As can be seen from Figure 4 $\theta_* = -0.002$ K is found to best fit the observed θ curve in the surface layer. However, since Ψ_h is positive but smaller than $\ln(z/z_0)$ this θ_* may be regarded a lower limit and a slightly larger θ_* not larger by a factor of 2 may be realistic.

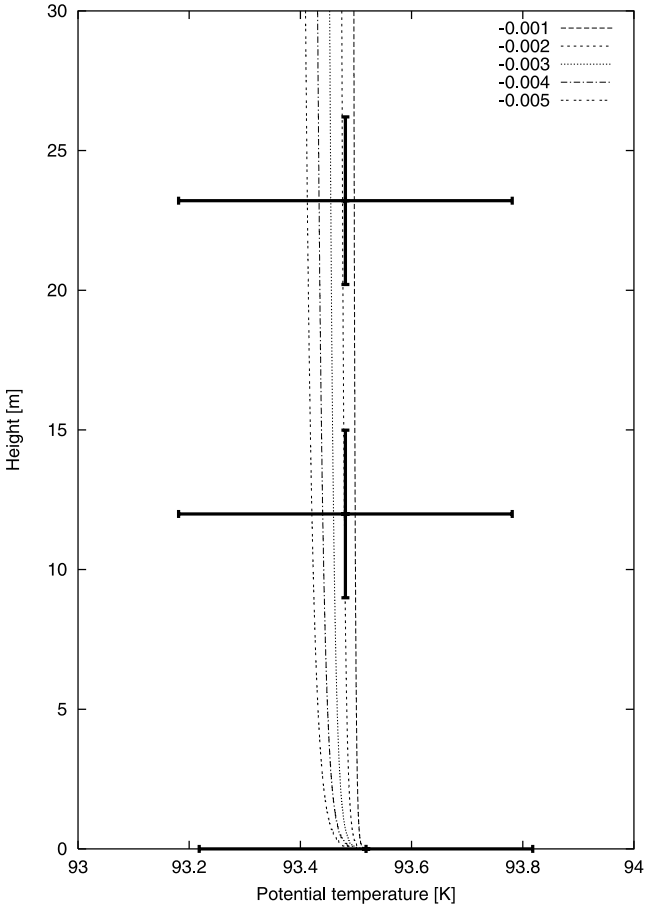

Figure 4. Vertical profile of potential temperature near the surface along with the logarithmic potential temperature profile (equation (10)) for different turbulent temperature scales θ_*. The data are shown as points with error bars; $\theta_* = -0.002$ K can best reproduce the observed data.

[37] The kinematic heat flux is given by

$$Q = -\overline{w'\theta'} = u_*\theta_* \tag{11}$$

Using u_* from section 3.3, Q is determined as 3.7×10^{-6} K m s^{-1}. This can also be expressed in energetic units (sensible heat flux) as $H_S = Qc_p\rho = 0.02$ W m^{-2}. The upward heat flux indicates that the ground surface temperature was slightly higher than the air temperature immediately above the surface. The heat flux at Titan's surface is smaller than in the equatorial regions of the Earth ($\sim$200 W m^{-2}) [*Arya*, 2001] or Mars ($\sim$10 W m^{-2}) [*Zurek et al.*, 1992] by several orders of magnitude. The radiative-convective model for Titan of *McKay et al.* [1991] predicted a surface heat flux of

0.037 W m^{-2} corresponding to roughly 1% of the global mean incident solar flux. The radiative-convective grey atmosphere model of *Lorenz and McKay* [2003] predicted a surface heat flux of 0.02 W m^{-2} corresponding to 0.5% of the incident solar flux. Both estimations nicely agree with our value within the estimated error.

4.2. Diurnal Variation of the PBL

[38] One important characteristic that is not readily visible in the instantaneous vertical θ profile is the extent of a diurnal variation in the vertical heat flux at the surface and within the PBL in the form of sensible heat flux. Basically the observed θ profile (Figure 2) could also be consistent with a transient feature in the morning, given its resemblance to similar θ profiles in the terrestrial PBL in the morning. However, considering the weak solar flux on Titan's surface we also have to consider a case in which the observed profile is a steady state permanent feature without a diurnal cycle.

[39] The presence or absence of a diurnal variation in the PBL structure at the Huygens landing site can be examined by analyzing the vertical heat flux between the surface and atmosphere that manifests itself in the θ profile. If we hypothetically assume that the convective PBL was growing because of surface heating in the morning, the time-integrated kinematic heat flux $Q_{int} = \int_0^t \overline{w'\theta'}\, dt$ can be determined by the area in the θ profile bounded by θ and the downward extrapolation of the θ gradient in the free atmosphere between the top of the PBL and surface, and is described [*Garratt*, 1992, equation (6.22)] by

$$Q_{int} = 0.5\gamma D^2 \tag{12}$$

where $\gamma \sim 4 \times 10^{-4}$ K m^{-1} is the vertical gradient of potential temperature mentioned in section 2.2 and D is the PBL depth. The time-integrated kinematic surface heat flux between sunrise and the time of Huygens landing turns out to be $Q_{int} \sim 18$ K m.

[40] Considering the instantaneous kinematic surface heat flux of 3.7×10^{-6} K m s^{-1} from the previous subsection some 5×10^6 s would be necessary to provide the total heat flux. However, sunrise took place only 2.77×10^5 s before Huygens landing. Moreover, the heat flux earlier in the morning is likely to be weaker than at the local time of landing. Therefore it appears unlikely that a convective PBL as deep as 300 m can be an immediate result of morning heating.

[41] The diurnal evolution of the convective mixed layer can also be estimated from the variation in the surface sensible heat flux using a thermodynamic model [*Arya*, 2001]

$$D = \left[D_0^2 + \frac{2}{\gamma} 1.2Q(LT - LT_0) \right]^{0.5} \tag{13}$$

where D_0 is the PBL depth at a given local time LT_0 and LT is the instantaneous local time.

[42] The diurnal wave of the kinematic heat flux can be parameterized as a function of solar local time as

$$Q = Q_{\max} \sin\left[\frac{\pi(LT - 6)}{12} \right] \tag{14}$$

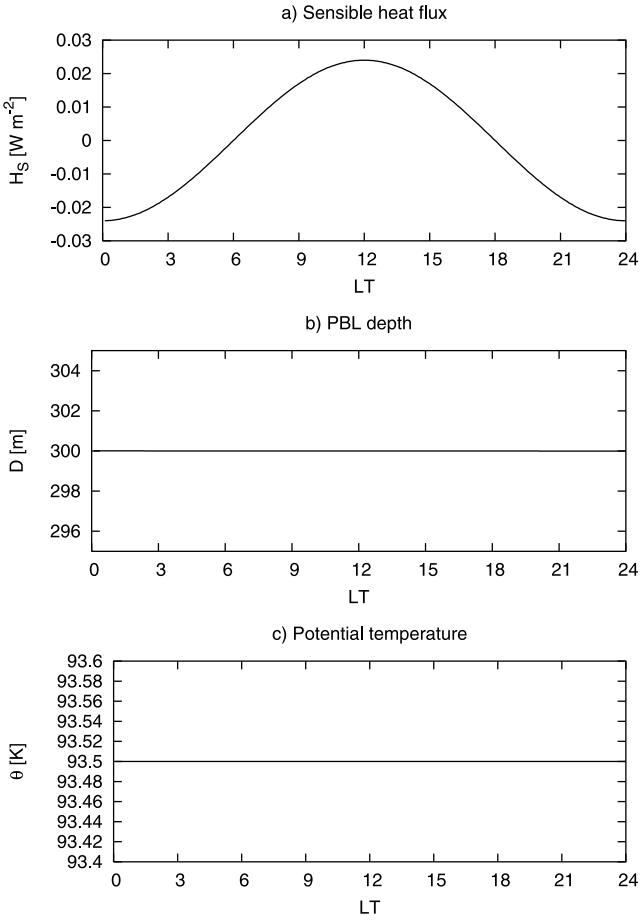

Figure 5. Diurnal variation in several PBL parameters simulated by a simple thermodynamic model of mixed-layer growth. (a) Sensible heat flux. Positive value indicates upward flux from the surface to atmosphere. (b) PBL depth. (c) Height-independent potential temperature of the mixed layer. The model is constrained by instantaneous values at the time of landing. The time axis is shown in units of local true solar time [*Allison et al.*, 2004] at the Huygens landing site.

where $Q_{\max}$ is the diurnal maximum of Q. $Q_{\max}$ is chosen such that the instantaneous value of Q at the local time of Huygens landing equals the value derived in section 4.1.

[43] The model results shown in Figure 5 clearly indicate that the tiny surface heat flux on Titan is not sufficient at all to cause a diurnal variation. The PBL depth changes by only 1 cm during one Titan day and the change in the potential temperature is smaller than it could be resolved by HASI temperature sensors. The negligible diurnal variation in the PBL depth can be regarded as the reason for the absence of a capping inversion at the top of the PBL (Figure 2).

5. Nature of Turbulence in the PBL

[44] In this section we estimate the strength of atmospheric turbulence in the PBL at the Huygens landing site using several parameters derived above. The turbulent kinetic energy (TKE) is a measure of the intensity of turbulence, and is directly related to the momentum or heat transport

through the PBL. The two major mechanisms to generate TKE in the PBL are the mechanical production by vertical wind shear and buoyant production by heat [e.g., *Stull*, 1988].

[45] The shear production of TKE is defined as

$$S = \overline{u'w'}\frac{\partial u}{\partial z} \tag{15}$$

where $\overline{u'w'}$ can be approximated by $K\frac{\partial u}{\partial z}$ and K is the eddy diffusivity derived in section 3.1.

[46] The buoyancy production term B is defined as

$$B = \frac{g}{T}\overline{w'\theta'} \tag{16}$$

where $\overline{w'\theta'}$ is the turbulent heat flux derived in section 4.1 and g = 1.354 m s^{-2} is the gravitational acceleration at Titan's surface.

[47] Figure 6 shows a comparison of the vertical profile of B and S in the surface layer for which we have an estimate of all the necessary PBL parameters required for calculating these TKE production terms. If the similarity function Ψ_m is neglected in the wind profile, the shear production term dominates in the lowest 1.5 m, but this term rapidly declines with altitude, and becomes insignificant at higher altitudes compared with the buoyancy production term. If instead Ψ_m is included, the crossover of the two terms takes place at a much lower altitude, i.e., near 0.3 m which corresponds to the Obukhov length L. The wind profile above 10 m is beyond the scope of this paper, but as a rule the shear production term of TKE is generally largest immediately above the surface, where the wind has to vanish [*Stull*, 1988]. The buoyant production term is only 5×10^{-7} m^2 s^{-3}. For comparison the corresponding typical value in terrestrial convective PBL on a sunny day is 10^{-3} to 10^{-2} m^2 s^{-3} [*Stull*, 1988], i.e., several orders of magnitude larger than on Titan. This illustrates that the turbulence caused by the heating of the surface of Titan is tiny.

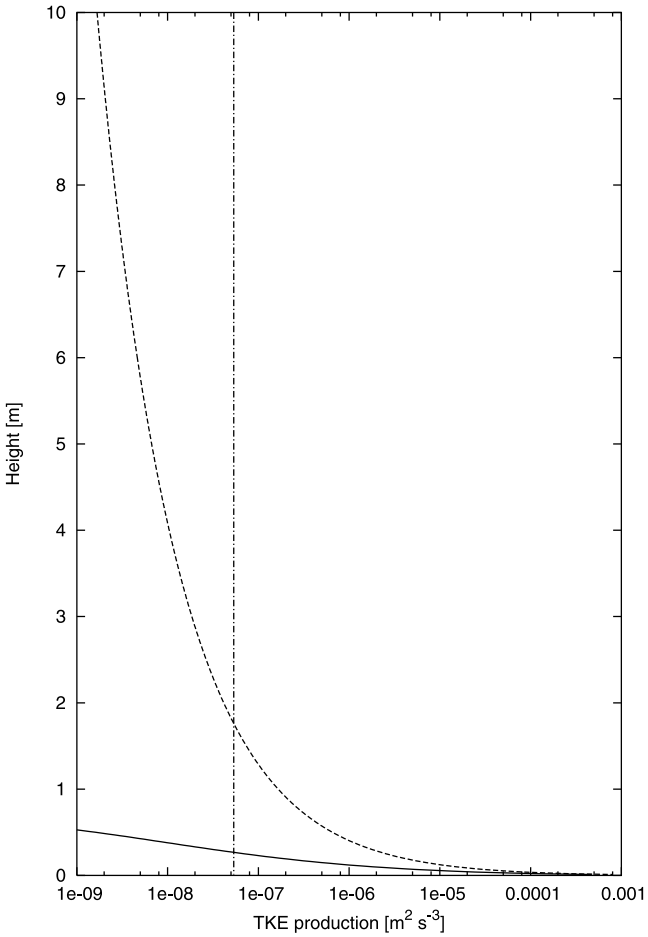

Figure 6. Vertical profile of shear production and buoyancy production terms of the turbulent kinetic energy in the surface layer. The dashed line is the S term for the pure logarithmic wind profile, the solid line is the S term for the wind profile corrected with the similarity function (as in Figure 3), and the vertical dash-dotted line is the B term.

6. Meteorological Interpretation of the PBL Data

[48] The PBL observed at the Huygens landing site can be classified as a convective (unstable) PBL, albeit the instability is tiny. The presence of such a PBL without significant convective or stable stratification on Titan is an immediate consequence of the weak sunlight at Titan's surface. The resulting small diurnal variation in the ground surface temperature can create only a minor temperature difference between the surface and atmosphere at any time, so the surface heat flux responsible for the heating or cooling of the atmosphere from below is always quite limited. In combination with the huge radiative time constant in Titan's troposphere large diurnal variations in near-surface temperature cannot be expected at all.

[49] Although a quite calm weather condition is implied, the observed structure should be clearly distinguished from a terrestrial winter-type PBL, i.e., stable PBL with a substantial inversion layer near the surface. Despite weak sunlight the landing site is illuminated for half a Titan day (8 Earth days), in stark contrast to the polar night in which the strong cooling of the surface generates a near-surface inversion layer and stable stratification.

[50] The thermal structure of the PBL revealed by Huygens is largely consistent with previous expectation and model results for the equatorial region. Virtually all Titan GCMs predicted in the equatorial regions lapse rates close to the adiabatic one in the lowest few kilometers for all seasons. More variable are the model predictions concerning the polar region not measured by Huygens. In the GCM of *Tokano* [2005] the seasonal cycle in the insolation caused a seasonal variation in the surface temperature by a few K, somewhat depending on the assumed surface thermal properties. In the case of solid surface the summer pole turned out to be the warmest place Titan-wide and the correlation of the predicted superadiabatic lapse rates and the occurrence of convective clouds near the summer pole [*Brown et al.*, 2002] was pointed out [*Tokano*, 2005]. The opposite, winter pole exhibited a weak inversion layer with a temperature increase with altitude near the surface. On the other hand, another series of Titan GCMs [*Rannou et al.*, 2004, 2006] predicted that the near-surface

temperature barely changes with season. The equatorial region is always warmest and the temperature decreases by about 3 K toward the poles. This difference is explained by the permanent accumulation of haze particles in the polar region, giving rise to a greatly subdued solar flux near the poles even in high summer.

[51] This difference in the predicted PBL structure in the polar region, particularly in summer, would have a significant impact on our understanding of Titan's tropospheric meteorology. If the near-surface temperature increases monotonically from the winter pole to summer pole, as predicted by *Tokano* [2005], this would indicate via thermal wind relation that the zonal wind is retrograde in summer and prograde in winter [*Tokano and Neubauer*, 2005]. The strength of seasonal temperature variation in the PBL affects the zonal wind direction, which in turn gives rise to angular momentum exchange between the surface and atmosphere and eventually Titan's length of day [*Tokano and Neubauer*, 2005]. If instead the near-surface temperature is permanently symmetric about the equator, as predicted by *Rannou et al.* [2004, 2006], the zonal wind would be prograde both in winter and summer considering the thermal wind relation.

[52] The second importance of the seasonal variation in the PBL temperature at high latitudes concerns the mechanism of tropospheric clouds observed on Titan. *Brown et al.* [2002] proposed that convective clouds may develop near the summer pole as a result of surface heating. This mechanism requires superadiabatic lapse rates in the lowest few kilometers, which indeed are predicted to exist near the summer solstice in the polar region [*Tokano*, 2005]. However, this mechanism can barely explain rapidly evolving clouds recently observed at southern midlatitudes [*Griffith et al.*, 2005; *Roe et al.*, 2005]. *Rannou et al.* [2006] proposed a different scenario for the same cloud observations on the basis of their GCM with a coupled methane-ethane cloud microphysics. According to their model prediction thick clouds near the summer pole naturally develop by slanted rising motion of methane in an oblique meridional cell into the cold polar region. In contrast to the above hypothesis the thermal stratification at the summer pole is stable, so convection was not possible. Unfortunately, the PBL data from HASI cannot constrain the vertical temperature profile in the polar region and thus the mechanism of cloud development.

7. Conclusions

[53] HASI performed the first in situ measurement of the temperature and pressure down to the surface of Titan with a vertical resolution sufficient to analyze the vertical structure of the PBL. The HASI measurements provide the first 'ground truth' and so far the best data on Titan's PBL. The high accuracy of the data enabled us to extract relevant information on the instantaneous thermal structure as well as diurnal variation. No remote sensing instrument is expected to yield a comparable resolution in the PBL. After Earth and Mars, Titan is the third place in the solar system in which the validity of boundary layer meteorology can be tested.

[54] The potential temperature profile reveals the existence of a slightly convective but close to neutral PBL with a depth of about 300 m, of which the surface layer constitutes the lowest 10 m. The decrease of potential temperature near the surface indicates upward flux of heat at the surface, but the derived heat flux is too small to cause a diurnal variation in the PBL depth. The derived eddy diffusion coefficient of less than 10^{-2} m^2 s^{-1} suggests that the turbulence in Titan's PBL is quite weak, at least at the landing site. The mean wind speed near the surface is likely to be less than 0.1 m s^{-1}. The turbulence in the PBL is tiny by terrestrial standards, mainly as a result of weak heating of the surface. Otherwise HASI did not detect any qualitatively unexpected structure of the PBL on Titan.

[55] Despite its relevance for the understanding of Titan's climate, dynamic meteorology and cloud microphysics the characteristics of the PBL at high latitudes cannot be examined on the basis of our data. Besides seasonal and latitudinal variation geographical variation may also exist given the vast heterogeneity of Titan's surface that is being revealed by Cassini [e.g., *Elachi et al.*, 2005; *Porco et al.*, 2005; *Sotin et al.*, 2005; *Barnes et al.*, 2005]. Topography or roughness of the surface are relevant factors affecting the PBL structure, such as the roughness length z_0, surface drag coefficient C_D or friction speed u_*.

[56] The wind profile is another major means of characterizing the PBL. Moreover, aeolian erosion has been considered long before [*Lorenz et al.*, 1995] and tentatively suggested by several Cassini teams [*Porco et al.*, 2005] to explain some of the observed surface features on Titan, calling for a detailed knowledge of the atmospheric structure close to the surface. However, the temperature and pressure data acquired by HASI do not allow a comprehensive analysis of the wind structure. A combined study with the wind data measured by other Huygens instruments (DWE and DISR) and the descent trajectory working group (DTWG) holds promise for a further insight into the PBL structure of Titan.

[57] **Acknowledgments.** T.T. was supported by a grant from the DFG within the priority program "Mars and the terrestrial planets" (SPP 1115). The Cassini-Huygens mission is a cooperative project of NASA, the European Space Agency (ESA), and the Italian Space Agency (ASI). The Huygens Atmospheric Structure Instrument (HASI), provided by ASI to the Huygens probe, is a multisensor package designed to measure the physical quantities characterizing Titan's atmosphere. HASI has been realized and operated by CISAS under a contract with the Italian Space Agency (ASI) within an international collaboration.

References

Allison, M. (1992), A preliminary assessment of the Titan planetary boundary layer, in *Proceedings of the Symposium on Titan, Toulouse, France, 9–12 September 1991*, edited by B. Kaldeich, *Eur. Space Agency Spec. Publ., ESA SP-338*, 113–118.

Allison, M., D. H. Atkinson, M. K. Bird, and M. G. Tomasko (2004), Titan zonal wind corroboration via the Huygens DISR solar zenith angle measurement, in *Proceedings of the International Workshop on Planetary Probe Atmospheric Entry and Descent Trajectory Analysis and Science, Lisbon, Portugal, 6–9 October 2003*, edited by A. Wilson, *Eur. Space Agency Spec. Publ., ESA SP-544*, 125–130.

Arya, S. P. (2001), *Introduction to Micrometeorology*, Elsevier, New York.

Barnes, J. W., et al. (2005), A 5-micron-bright spot on Titan: Evidence for surface diversity, *Science*, *310*, 92–95.

Bird, M. K., et al. (2005), The vertical profile of winds on Titan, *Nature*, *438*, 800–802.

Brown, M. E., A. H. Bouchez, and C. A. Griffith (2002), Direct detection of variable tropospheric clouds near Titan's south pole, *Nature*, *420*, 795–797.

Elachi, C., et al. (2005), Cassini radar views the surface of Titan, *Science*, *308*, 970–974.

Flasar, F. M., R. E. Samuelson, and B. J. Conrath (1981), Titan's atmosphere: Temperature and dynamics, *Nature*, *292*, 693–698.

Fulchignoni, M., et al. (2005), In situ measurements of the physical characteristics of Titan's environment, *Nature*, *438*, 785–791.
Garratt, J. R. (1992), *The Atmospheric Boundary Layer*, Cambridge Univ. Press, New York.
Griffith, C. A., et al. (2005), The evolution of Titan's mid-latitude clouds, *Science*, *310*, 474–477.
Haltiner, G. J., and R. T. Williams (1980), *Numerical Prediction and Dynamic Meteorology*, John Wiley, Hoboken, N. J.
Hinson, D. P., and G. L. Tyler (1983), Internal gravity waves in Titan's atmosphere oberved by Voyager radio occultation, *Icarus*, *54*, 337–352.
Larsen, S. E., H. E. Jørgensen, L. Landberg, and J. E. Tillman (2002), Aspects of the atmospheric surface layers on Mars and Earth, *Boundary Layer Meteorol.*, *105*, 451–470.
Lebreton, J. P., et al. (2005), An overview of the descent and landing of the Huygens probe on Titan, *Natures*, 758–764.
Lettau, H. (1969), Note on aerodynamic roughness-parameter estimation on the basis of roughness-element distribution, *J. Appl. Meteorol.*, *8*, 820–832.
Lindal, G. F., G. E. Wood, H. B. Hotz, D. N. Sweetnam, V. R. Eshleman, and G. L. Tyler (1983), The atmosphere of Titan—An analysis of the Voyager 1 radio occultation measurements, *Icarus*, *53*, 348–363.
Linkin, V. M., et al. (1986), Vertical thermal structure in the Venus atmosphere from provisional Vega 2 temperature and pressure data, *Sov. Astron. Lett., Engl. Transl.*, *12*, 40–42.
Lorenz, R. D. (2006), Thermal interactions of the Huygens probe with the Titan environment: Constraint on near-surface wind, *Icarus*, *182*, 559–566.
Lorenz, R. D., and C. P. McKay (2003), A simple expression for vertical convective fluxes in planetary atmospheres, *Icarus*, *165*, 407–413.
Lorenz, R. D., J. I. Lunine, J. A. Grier, and M. A. Fisher (1995), Prediction of aeolian features on planets: Application to Titan paleoclimatology, *J. Geophys. Res.*, *100*(E12), 26,377–26,386.
Mäkinen, T. (1996), Processing the HASI measurements, *Adv. Space Res.*, *17*(11), 217–222.
McKay, C. P., J. B. Pollack, and R. Courtin (1991), The greenhouse and antigreenhouse effects on Titan, *Science*, *253*, 1118–1121.
Niemann, H. B., et al. (2005), The abundances of constituents of Titan's atmosphere from the GCMS instrument on the Huygens probe, *Nature*, *438*, 779–784.
Porco, C. C., et al. (2005), Imaging of Titan from the Cassini spacecraft, *Nature*, *434*, 159–168.
Rannou, P., F. Hourdin, C. P. McKay, and D. Luz (2004), A coupled dynamics-microphysics model of Titan's atmosphere, *Icarus*, *170*, 443–462.
Rannou, P., F. Montmessin, F. Hourdin, and S. Lebonnois (2006), The latitudinal distribution of clouds on Titan, *Science*, *311*, 201–205.
Roe, H. G., M. E. Brown, E. L. Schaller, A. H. Bouchez, and C. A. Trujillo (2005), Geographic control of Titan's mid-latitude clouds, *Science*, *310*, 477–479.
Smith, M. D., et al. (2004), First atmospheric science results from the Mars Exploration Rovers Mini-TES, *Science*, *306*, 1750–1753.
Sotin, C., et al. (2005), Release of volatiles from a possible cryovolcano from near-infrared imaging of Titan, *Nature*, *435*, 786–789.
Stull, R. B. (1988), *An Introduction to Boundary Layer Meteorology*, Springer, New York.
Tokano, T. (2005), Meteorological assessment of the surface temperatures on Titan: Constraints on the surface type, *Icarus*, *173*, 222–242.
Tokano, T., and F. M. Neubauer (2002), Tidal winds on Titan caused by Saturn, *Icarus*, *158*, 499–515.
Tokano, T., and F. M. Neubauer (2005), Wind-induced seasonal angular momentum exchange at Titan's surface and its influence on Titan's length-of-day, *Geophys. Res. Lett.*, *32*, L24203, doi:10.1029/2005GL024456.
Tomasko, M. G., et al. (2005), Rain, wind and haze during the Huygens probe's descent to Titan's surface, *Nature*, *438*, 765–778.
West, R. A., M. E. Brown, S. V. Salinas, A. H. Bouchez, and H. G. Roe (2005), No oceans on Titan from the absence of a near-infrared specular reflection, *Nature*, *436*, 670–672.
Zarnecki, J. C., et al. (2005), A soft solid surface on Titan as revealed by the Huygens surface science package, *Nature*, *438*, 792–795.
Zurek, R. W., J. R. Barnes, R. M. Haberle, J. B. Pollack, J. E. Tillman, and C. B. Conway (1992), Dynamics of the atmosphere of Mars, in *Mars*, edited by H. H. Kieffer et al., pp. 835–933, Univ. of Ariz. Press, Tucson.

G. Colombatti and F. Ferri, CISAS "G. Colombo," Università di Padova, Via Venezia 15, I-35131 Padova, Italy.
M. Fulchignoni, LESIA, Observatoire de Paris, 5 Place Jules Janssen, F-92195 Meudon, France.
T. Mäkinen, Finnish Meteorological Institute, Geophysical Research, P. O. Box 503, FIN-00101 Helsinki, Finland.
T. Tokano, Institut für Geophysik und Meteorologie, Universität zu Köln, Albertus-Magnus-Platz, D-50923 Köln, Germany. (tokano@geo.uni-koeln.de)